Acta Crystallographica Section F
Structural Biology Communications
ISSN 2053-230X

Crystallization and preliminary X-ray diffraction analysis of the Sel1-like repeats of SEL1L

Hanbin Jeong, Hakbong Lee and Changwook Lee*

School of Life Sciences, Ulsan National Institute of Science and Technology, 50 UNIST-gil, Eonyang-eup, Ulju-gun, Ulsan 689-798, Republic of Korea

Correspondence e-mail: changwook@unist.ac.kr

Received 5 September 2014
Accepted 20 October 2014

Terminally misfolded or unassembled proteins are selectively recognized and cleared by the ER-associated degradation (ERAD) pathway. Suppressor/enhancer of lin-12-like (SEL1L), a component of the dislocation machinery containing the E3 ubiquitin ligase Hrd1, plays an important role in selecting and transporting ERAD substrates for degradation in the endoplasmic reticulum. In this study, the purification, crystallization and preliminary X-ray diffraction analysis of recombinant mouse SEL1L (residues 348–533) are reported. The crystals were obtained by the hanging-drop vapour-diffusion method at pH 8.5 and 277 K using 30% 2-propanol as a precipitant. Optimized crystals diffracted to 3.3 Å resolution at a synchrotron-radiation source. Preliminary X-ray diffraction analysis revealed that the crystals belonged to space group $P2_1$ and contained four molecules per asymmetric unit, with a solvent content of 44%.

1. Introduction

The endoplasmic reticulum (ER) serves many general functions including the folding of proteins and the transportation of synthesized proteins in vesicles to the Golgi apparatus, as well as cellular protein quality control (Ellgaard & Helenius, 2003; Vembar & Brodsky, 2008). Terminally misfolded or unassembled secretory proteins are destroyed by an ubiquitin-dependent proteosomal degradation process known as ER-associated degradation (ERAD; Plemper & Wolf, 1999; Tsai *et al.*, 2002; Hirsch *et al.*, 2009). ERAD is a conserved system from yeast to mammals, suggesting that it is an essential process for protein quality control in the cell. To date, many components involved in the ERAD process, including Hrd1, SEL1L (Hrd3p), the ERAD lectin Os9, the membrane-spanning Derlin-1/2, VIMP and Herp (US1), have been identified through genetic and biochemical analyses in yeast and mammals (Christianson & Ye, 2014). Among the essential components, Hrd1 is an E3 ubiquitin ligase and is located in the ER membrane through multiple transmembrane domains. Hrd1 is involved in the retrotranslocation of substrates, as well as in the ubiquitination of substrates by a cytosolic RING finger domain (Bays *et al.*, 2001; Deak & Wolf, 2001). Os9 is an ER-resident protein that binds to ERAD substrates and recruits the substrates to the membrane-embedded Hrd1–SEL1L complex (Christianson *et al.*, 2008). SEL1L, the homologue of yeast Hrd3p, functions as a scaffold, interacting between the substrate-recognized Os9 and Hrd1 in translocating ERAD substrates to be selectively degraded (Mueller *et al.*, 2006). Recent studies have shown that SEL1L critically determines the stability of the Hrd1–SEL1L complex to optimize the degradation kinetics of ERAD substrates (Iida *et al.*, 2011). The physiological roles of SEL1L have recently been studied using inducible SEL1L knockout mouse and cell models, elucidating that SEL1L is essential for mammalian endoplasmic reticulum-associated degradation, endoplasmic reticulum homeostasis and cell survival (Sun *et al.*, 2014).

SEL1L is a type I membrane protein with a single transmembrane domain at the C-terminus, embedded in the ER membrane, and has a large luminal domain. From the primary structure of SEL1L, it was predicted that the luminal domain of SEL1L contains a couple of Sel1-like repeats (Biunno *et al.*, 2006). A Sel1-like repeat is a

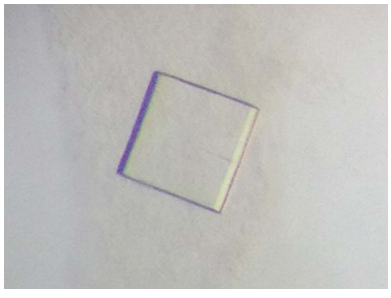

Table 1
Macromolecule-production information.

Source organism	*M. musculus*
DNA source	Kidney cDNA
Forward primer	5′-GCCGGATCCAACAGTGGGATGCTGGAAGAA-3′
Reverse primer	5′-GCCGGTCGACCTACCGCATCACCCCTGTGCC-3′
Expression vector	pET-28b-smt3
Expression host	*E. coli* BL21 (DE3)
UniProt accession No.	Q9Z2G6

structural motif that closely resembles a tetratricopeptide repeat (TPR), which consists of two helices connected by a short loop, and this hairpin-like structure is known to generally contribute to protein–protein interaction modules (Das *et al.*, 1998; Lüthy *et al.*, 2002; Mittl & Schneider-Brachert, 2007). In order to clearly understand the biochemical role of the Sel1-like repeats of SEL1L in ER-associated proteasomal degradation, it is essential to determine the atomic resolution structure of SEL1L. In this study, we report the purification and preliminary X-ray crystallographic analysis of the highly conserved Sel1-like repeats of mouse SEL1L comprising residues 348–533 (hereafter referred to as SEL1L$^{\rm trunc}$). Based on this analysis, we attempted to solve the three-dimensional structure of SEL1L.

2. Materials and methods

2.1. Macromolecule production

The gene encoding SEL1L (residues 348–533) was amplified from mouse kidney cDNA using PCR with the following primers: forward, 5′-GCCGGATCCAACAGTGGGATGCTGGAAGAA-3′; reverse, 5′-GCCGGTCGACCTACCGCATCACCCCTGTGCC-3′. The amplified gene was digested with the restriction enzymes *Bam*HI and *Sal*I at the N-terminus and C-terminus, respectively, and was ligated into pET-28b-smt3 vector to produce an N-terminal histidine-smt3 fusion protein. This construct encoded a His$_6$-smt3-SEL1L$^{\rm trunc}$ protein with an Ulp1 protease recognition sequence between smt3 and SEL1L$^{\rm trunc}$.

The plasmid encoding His$_6$-smt3-SEL1L$^{\rm trunc}$ was transformed into *Escherichia coli* strain BL21 (DE3) cells for protein expression. A 3 ml seed from an overnight culture was subcultured into 1000 ml fresh Luria–Bertani (LB) medium containing the antibiotic kanamycin (50 µg ml^{-1}). When the cell density reached an OD$_{600}$ of 0.5–0.8, isopropyl β-D-1-thiogalactopyranoside was added to a final concentration of 0.2 m*M*. The cells were further cultured at 291 K for 20 h and harvested by centrifugation. The cells were resuspended in buffer *A* (25 m*M* sodium phosphate, 400 m*M* NaCl, 10 m*M* imidazole pH 7.4) and lysed by sonication. After centrifugation for 50 min at 23 000*g*, the supernatant was loaded onto an Ni-charged chelating column (GE Healthcare) equilibrated with buffer *A*. After washing with buffer *B* (25 m*M* sodium phosphate, 400 m*M* NaCl, 50 m*M* imidazole pH 7.4), the bound SEL1L$^{\rm trunc}$ protein was eluted from the column using buffer *C* (25 m*M* sodium phosphate, 300 m*M* NaCl, 400 m*M* imidazole pH 7.4). The eluted protein was dialyzed against 25 m*M* Tris, 150 m*M* NaCl, 5 m*M* DTT pH 7.5 overnight to remove imidazole. The N-terminal His$_6$-smt3 tag was cleaved by Ulp1 protease at a ratio of 1:1000(*w*:*w*) Ulp1:His$_6$-smt3-SEL1L$^{\rm trunc}$ during dialysis. Dialyzed protein solution was loaded onto a Ni-charged chelating column again to remove the His$_6$-smt3 tag. The protein was further purified on a Superdex 200 16/60 gel-filtration column (GE Healthcare) equilibrated with 25 m*M* Tris, 150 m*M* NaCl, 5 m*M* DTT pH 7.5. The eluted SEL1L$^{\rm trunc}$ protein was finally concentrated to 20 mg ml^{-1} and flash-frozen in liquid nitrogen for storage. All purification steps were carried out at 277 K and monitored by SDS–PAGE (Fig. 1). The protein concentration was determined by direct UV measurement at 280 nm with a spectrophotometer (Ultrospec 2100 pro, GE Healthcare) using an extinction coefficient of 26 360 M^{-1} cm^{-1} as calculated using the *ProtParam* tool (ExPASy). Macromolecule-production information is summarized in Table 1.

Table 2
Data collection and processing.

Values in parentheses are for the highest resolution shell.

Beamline	7A, PAL
Wavelength (Å)	1.0000
Temperature (K)	100
Detector	ADSC Quantum 270 CCD
Rotation range per image (°)	1
Total rotation range (°)	170
Exposure time per image (s)	1
Space group	$P2_1$
a, b, c (Å)	29.60, 110.02, 109.74
α, β, γ (°)	90.00, 91.10, 90.00
Resolution range (Å)	50–3.3 (3.36–3.30)
Total No. of reflections	36917
No. of unique reflections	10661 (551)
Completeness (%)	99.8 (100.0)
Multiplicity	3.5 (3.5)
$\langle I/\sigma(I)\rangle$	16.2 (4.2)
$R_{\rm merge}$† (%)	10.2 (41.4)

† $R_{\rm merge} = 100 \times \sum_{hkl}\sum_i |I_i(hkl) - \langle I(hkl)\rangle|/\sum_{hkl}\sum_i I_i(hkl)$, where $I_i(hkl)$ is the ith measurement and $\langle I(hkl)\rangle$ is the weighted mean of all measurements of $I(hkl)$ for the reflection with Miller indices *hkl*.

2.2. Crystallization

Initial crystallization screening was performed at both 277 and 293 K by the hanging-drop vapour-diffusion method in a 24-well VDX crystallization plate (Hampton Research) using commercially available screening kits including Crystal Screen, Crystal Screen 2, Grid Screen (Hampton Research) and Wizard (Emerald BioSystems). Crystallization drops were prepared by mixing 1 µl of a 10 mg ml^{-1} protein solution in buffer (25 m*M* Tris, 150 m*M* NaCl, 5 m*M* DTT pH 7.5) and 1 µl well solution. Crystals of SEL1L$^{\rm trunc}$ were initially obtained using a well solution consisting of 30% 2-propanol, 100 m*M* NaCl, 100 m*M* Tris pH 8.5. The crystallization condition was optimized by varying the protein concentration, the

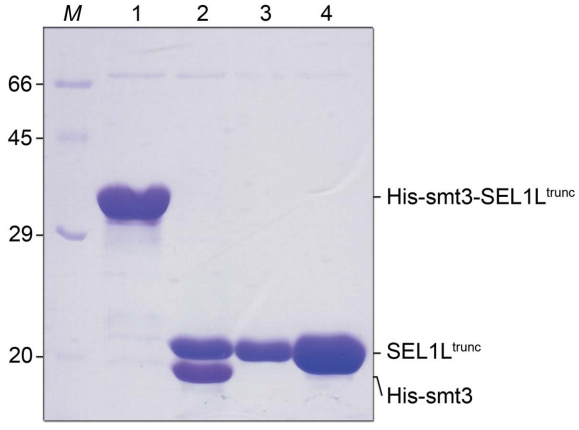

Figure 1
Protein purification. SDS–PAGE analysis showing the purification of recombinant SEL1L$^{\rm trunc}$; lane 1, His-smt3-fused SEL1L$^{\rm trunc}$ after nickel–IMAC chromatography; lane 2, Ulp1 digestion of His-smt3-fused SEL1L$^{\rm trunc}$; lane 3, SEL1L$^{\rm trunc}$ after the second nickel-IMAC step to remove His-smt3; lane 4, SEL1L$^{\rm trunc}$ after gel filtration. Lane *M* contains molecular-weight marker (AccuLadder Protein Size Marker, Bioneer; labelled in kDa).

precipitant concentration and the pH and by using Additive Screen (Hampton Research).

2.3. Data collection and processing

For diffraction studies, crystals were transferred to a cryoprotection solution containing paraffin oil and were flash-cooled in liquid nitrogen. X-ray data were collected from cooled crystals on beamline 7A of Pohang Accelerator Laboratory (PAL), Pohang, Republic of Korea. X-ray diffraction data were processed with *HKL*-2000 (Otwinowski & Minor, 1997). The data-collection statistics are summarized in Table 2.

3. Results and discussion

The *Mus musculus* SEL1L protein contains 790 amino acids. To obtain soluble and homogenous protein, we constructed a truncated version (residues 348–533) of mouse SEL1L (SEL1L^{trunc}). SEL1L^{trunc} was expressed as a His_6-smt3 fusion protein at the N-terminus and was purified to homogeneity. The purity of SEL1L^{trunc} in the final purification step was at least 95% as monitored by SDS–PAGE (Fig. 1). We obtained 10 mg pure protein per litre of bacterial culture broth. Crystals of SEL1L^{trunc} were initially obtained in a crystallization condition consisting of 30% 2-propanol, 100 m*M* NaCl, 100 m*M* Tris pH 8.5 at 277 K by the hanging-drop vapour-diffusion

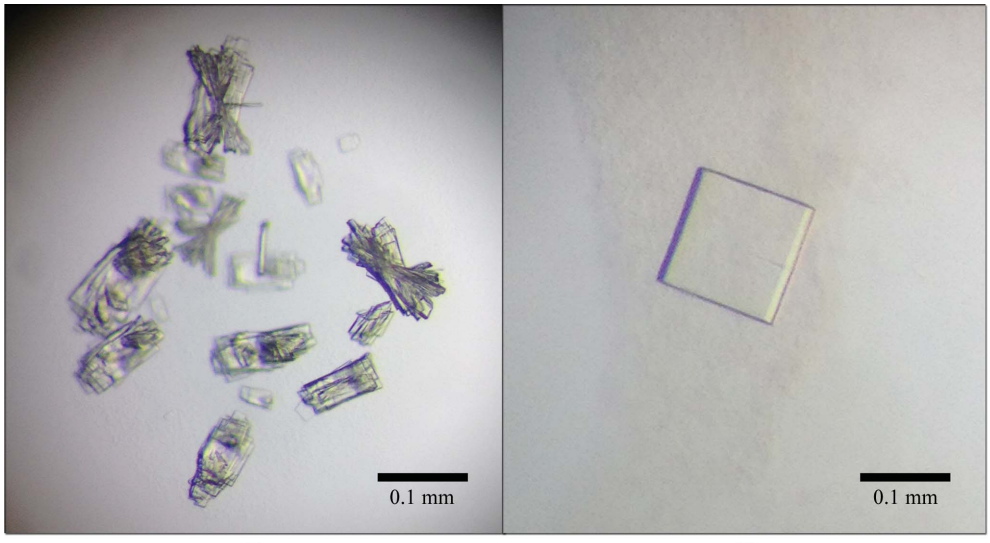

Figure 2
Crystals of mouse SEL1L^{trunc}. Crystals of mouse SEL1L^{trunc} grown in (*a*) the initial condition comprising 30% 2-propanol, 100 m*M* NaCl, 100 m*M* Tris pH 8.5 and (*b*) an improved condition comprising the initial condition plus 20 m*M* phenol and 5 m*M* DTT (maximum dimensions 0.1 × 0.1 × 0.01 mm).

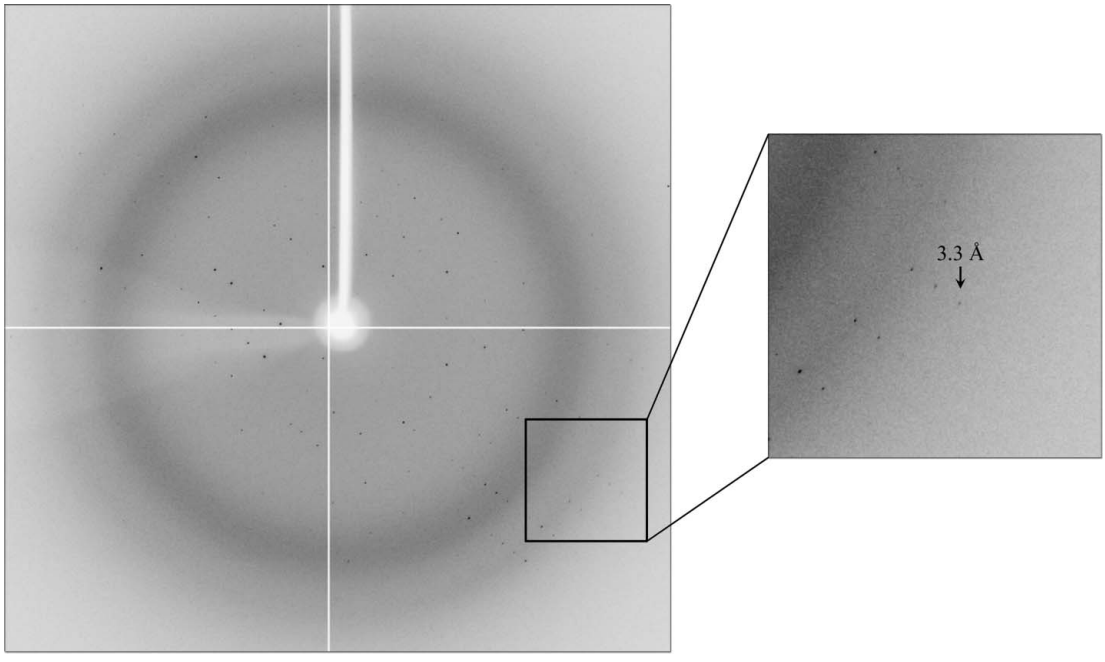

Figure 3
X-ray diffraction image. An X-ray diffraction pattern collected from a single crystal of SEL1L^{trunc}. The diffraction image was obtained using a synchrotron-radiation source. The maximum observed resolution is 3.3 Å.

method. We finally improved this condition to 30% 2-propanol, 100 m*M* NaCl, 100 m*M* Tris, 5 m*M* DTT, 20 m*M* phenol pH 8.5 in order to obtain the best diffracting crystals. A rectangular thin plate-shaped crystal of SEL1L^{trunc} appeared in 3–4 d and continued to grow in size over the following week (Fig. 2). When we turned over the cover glass to harvest the crystals, they kept spinning in the crystallization drop, most likely owing to the high concentration of 2-propanol used as a precipitant. To reduce the spinning turbulence of the crystals in the drop and to protect against crystal damage during cooling, we added paraffin oil to the crystallization drop and harvested the crystal rapidly using a cryo-loop followed by flash-cooling in liquid nitrogen. The SEL1L^{trunc} crystals displayed a good-quality diffraction pattern (Fig. 3). The crystals diffracted to 3.3 Å resolution using synchrotron radiation. The crystals belonged to space group $P2_1$, with unit-cell parameters a = 29.60, b = 110.02, c = 109.74 Å, α = 90.00, β = 91.10, γ = 90.00° (Table 2). Assuming the presence of four molecules per asymmetric unit, the Matthews coefficient (V_M) was estimated to be 2.18 Å^3 Da^{-1}, with a solvent content of 44% (Matthews, 1968). Although the unit-cell parameters implied the possibility that the space group of the crystals could be tetragonal, attempts to process the data in a tetragonal space group were unsuccessful. The mean R_{merge} values for space groups *P*422 and *P*4 were 43.3 and 49.5%, respectively. The correct space group ($P2_1$) of the crystals was confirmed by *POINTLESS* from the *CCP*4 suite and *phenix.xtriage* (Adams *et al.*, 2010; Evans, 2011; Winn *et al.*, 2011). Examination of the diffraction data with *phenix.xtriage* (Adams *et al.*, 2010) indicated that no twinning was found in the crystals. Molecular replacement was performed using the Sel1-like repeat-containing proteins HcpC (PDB entry 1ouv; Lüthy *et al.*, 2004) and c5321 (PDB entry 4bwr; Urosev *et al.*, 2013) as search models. However, no significant solutions could be found. Structure determination using SeMet-derivatized crystals of mouse SEL1L^{trunc} is in progress.

We thank the staff at beamline 7A of PAL for the use of and assistance with synchrotron facilities. This work was supported by the 2014 Research Fund (1.140023.01) of UNIST (Ulsan National Institute of Science and Technology). HJ was supported by the Global PhD Fellowship Program through the National Research Foundation of Korea (NRF) funded by the Ministry of Education (NRF-2014H1A2A1020322).

References

Adams, P. D. *et al.* (2010). *Acta Cryst.* D**66**, 213–221.
Bays, N. W., Gardner, R. G., Seelig, L. P., Joazeiro, C. A. & Hampton, R. Y. (2001). *Nature Cell Biol.* **3**, 24–29.
Biunno, I., Cattaneo, M., Orlandi, R., Canton, C., Biagiotti, L., Ferrero, S., Barberis, M., Pupa, S. M., Scarpa, A. & Ménard, S. (2006). *J. Cell. Physiol.* **208**, 23–38.
Christianson, J. C., Shaler, T. A., Tyler, R. E. & Kopito, R. R. (2008). *Nature Cell Biol.* **10**, 272–282.
Christianson, J. C. & Ye, Y. (2014). *Nature Struct. Mol. Biol.* **21**, 325–335.
Das, A. K., Cohen, P. W. & Barford, D. (1998). *EMBO J.* **17**, 1192–1199.
Deak, P. M. & Wolf, D. H. (2001). *J. Biol. Chem.* **276**, 10663–10669.
Ellgaard, L. & Helenius, A. (2003). *Nature Rev. Mol. Cell Biol.* **4**, 181–191.
Evans, P. R. (2011). *Acta Cryst.* D**67**, 282–292.
Hirsch, C., Gauss, R., Horn, S. C., Neuber, O. & Sommer, T. (2009). *Nature (London)*, **458**, 453–460.
Iida, Y., Fujimori, T., Okawa, K., Nagata, K., Wada, I. & Hosokawa, N. (2011). *J. Biol. Chem.* **286**, 16929–16939.
Lüthy, L., Grütter, M. G. & Mittl, P. R. E. (2002). *J. Biol. Chem.* **277**, 10187–10193.
Lüthy, L., Grütter, M. G. & Mittl, P. R. E. (2004). *J. Mol. Biol.* **340**, 829–841.
Matthews, B. W. (1968). *J. Mol. Biol.* **33**, 491–497.
Mittl, P. R. E. & Schneider-Brachert, W. (2007). *Cell. Signal.* **19**, 20–31.
Mueller, B., Lilley, B. N. & Ploegh, H. L. (2006). *J. Cell Biol.* **175**, 261–270.
Otwinowski, W. & Minor, W. (1997). *Methods Enzymol.* **276**, 307–326.
Plemper, R. K. & Wolf, D. H. (1999). *Trends Biochem. Sci.* **24**, 266–270.
Sun, S., Shi, G., Han, X., Francisco, A. B., Ji, Y., Mendoncca, N., Liu, X., Locasale, J. W., Simpson, K. W., Duhamel, G. E., Kersten, S., Yates, J. R. III, Long, Q. & Qi, L. (2014). *Proc. Natl Acad. Sci. USA*, **111**, 582–591.
Tsai, B., Ye, Y. & Rapoport, T. A. (2002). *Nature Rev. Mol. Cell Biol.* **3**, 246–255.
Urosev, D., Ferrer-Navarro, M., Pastorello, I., Cartocci, E., Costenaro, L., Zhulenkovs, D., Maréchal, J.-D., Leonchiks, A., Reverter, D., Serino, L., Soriani, M. & Daura, X. (2013). *BMC Struct. Biol.* **13**, 19.
Vembar, S. S. & Brodsky, J. L. (2008). *Nature Rev. Mol. Cell Biol.* **9**, 944–957.
Winn, M. D. *et al.* (2011). *Acta Cryst.* D**67**, 235–242.